Liquid Crystals
Publication details, including instructions for authors and subscription information:
http://www.informaworld.com/smpp/title~content=t713926090

Equal G analysis of ternary liquid-crystalline systems

Grant E. Nebel[a]; Gerald R. s. Van Hecke[a]
[a] Department of Chemistry, Harvey Mudd College, Claremont, California, U. S. A.

To cite this Article Nebel, Grant E. and Van Hecke, Gerald R. s.(1989) 'Equal G analysis of ternary liquid-crystalline systems', Liquid Crystals, 5: 2, 601 — 615
To link to this Article: DOI: 10.1080/02678298908045411
URL: http://dx.doi.org/10.1080/02678298908045411

LIQUID CRYSTALS, 1989, VOL. 5, NO. 2, 601–615

Equal G analysis of ternary liquid-crystalline systems

by GRANT E. NEBEL and GERALD R. VAN HECKE
Department of Chemistry, Harvey Mudd College, Claremont, California 91711, U.S.A.

The equal Gibbs energy analysis of binary liquid-crystalline systems can predict, to a high degree of accuracy, the phase diagram of the binary system. We extend this analysis to ternary systems. Two systems of homologous dialkyloxyazoxybenzenes were studied. In particular we studied the mixtures 6–1–5 and 6–4–5, where the number denotes the number of carbon atoms in the terminal alkyl chain. The experimental temperature–composition phase diagrams were determined by differential scanning calorimetry and by optical microscopy using a ternary contact method as well as individual compositions. Both the crystal–nematic and nematic–isotropic phase regions were studied. The first mixture is highly non-ideal, whereas the second is almost ideal. The form used for the excess Gibbs energy was

$$\Delta G^{E} = \Delta A_{12}\,xy + \Delta A_{23}\,y(1 - x - y) + \Delta A_{13}\,x(1 - x - y) + \Delta A_{123}\,xy(1 - x - y).$$

This particular form, where x, y and $(1 - x - y)$ are the molar fractions of the three components and A_{ijk} are the interaction parameters, either binary or ternary, looks at the origins of the excess Gibbs energies from the view of the three binary systems and a ternary perturbation. A method of treating ternary solid solution–liquid phase equilibria is introduced and discussed. The success of the method and the relative magnitudes and meanings of the parameters are discussed.

1. Introduction

Mixtures of liquid crystals have been, and continue to be, extensively studied. Very often such studies have been directed towards the analysis of binary isobaric temperature–composition phase diagrams. The analysis of phase diagrams is generally made by comparing what would be expected ideally with experiment. The difference between ideal and experiment is generally ascribed to the existence of non-idealities in the mixture. It is possible to quantify these non-idealities by calculating the Gibbs energy in excess expected ideal value.

We have applied a technique, drawn largely from the literature of materials science [1], called the equal G analysis, to the study of binary phase diagrams of liquid crystals [2]. The equal Gibbs energy analysis allows the quantitative calculation of the excess energy of a system from its phase diagram. This excess Gibbs energy must arise from the intermolecular forces present in the mixture of materials and is a quantitative description of those intermolecular forces. Our objects in this study were two-fold: first, to extend the applicability of the equal G analysis to ternary systems and, secondly, to make the first attempts at understanding the nature and magnitude of the liquid phase intermolecular forces present in two ternary systems each exhibiting nematic phases. Specifically, we studied mixtures of homologous 4,4′-di-*n*-alkyloxyazoxybenzenes whose pure and binary phase behaviours were well known. [3–5].

0267-8292/89 $3.00

2. Theory

The Gibbs potential for any phase under constant pressure may be expressed as a weighted sum of the individual chemical potentials of all components in the phase. For the ternary systems under study here, the molar fraction of components 1 and 2 will be designated x and y, respectively. The molar fraction of the third component depends on the first two and is written as $1 - x - y$. The equal G analysis begins by setting equal the total Gibbs potential of each phase. The isobaric locus of temperature and composition points where the Gibbs potentials of phases α and β are equal is defined by

$$x_\alpha\mu_{1\alpha} + y_\alpha\mu_{2\alpha} + (1 - x_\alpha - y_\alpha)\mu_{3\alpha} = x_\beta\mu_{1\beta} + y_\beta\mu_{2\beta} + (1 - x_\beta - y_\beta)\mu_{3\beta}. \quad (1)$$

Denoting the equal G compositions as x and y such that $x_\alpha = x_\beta = x$, $y_\alpha = y_\beta = y$, equation (1) becomes

$$x(\mu_{1\beta} - \mu_{1\alpha}) + y(\mu_{2\beta} - \mu_{2\alpha}) + (1 - x - y)(\mu_{3\beta} - \mu_{3\alpha}) = 0. \quad (2)$$

We note that solutions to equation (2) at a fixed temperature define the equal G compositions at that temperature and are represented graphically by the broken line in figure 1. The equal G values will always lie between x_α and x_β, y_α and y_β.

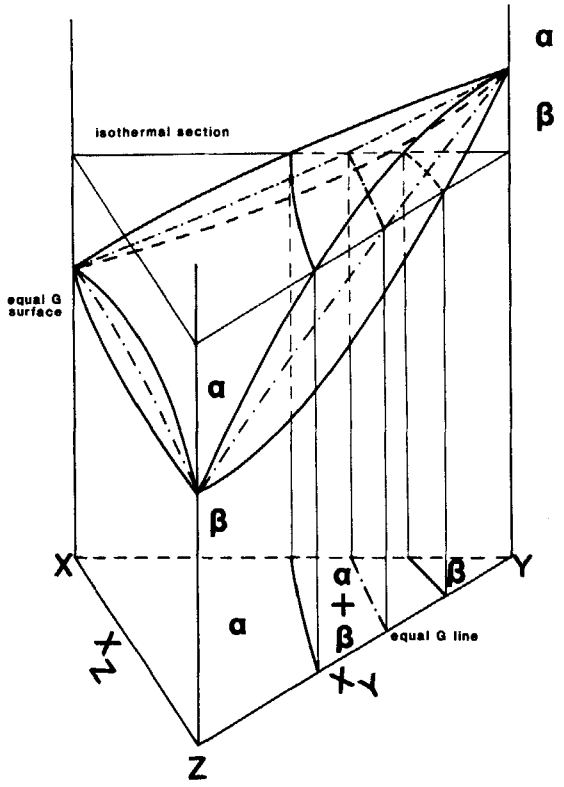

Figure 1. Idealized Gibbs energy surfaces for two phases α and β in equilibrium under isobaric and isothermal conditions. The broken line shows the locus of the equal Gibbs intersections which are always found between the equilibrium compositions that are determined by the locus of double tangent points. The projection shows the typical isothermal, isobaric ternary phase diagram with the equal Gibbs line depicted by —·—. (Adapted from figure X-4 of [6].)

The chemical potential difference for a component i between phase α and β is

$$\Delta\mu_i = -\Delta\bar{S}_i(T - T_i) + \Delta\mu_i^E, \tag{3}$$

where $\Delta\bar{S}_i$ is the molar entropy difference between the α and β phases at the pressure and the standard transition temperature T_i. The first term on the right may be called the ideal term resulting from a simple first order phase transition. The second term, if non-zero, accounts for the failure of the ideal term to describe adequately the true chemical potential difference. Moreover, equation (3) assumes a finite entropy change for the transition and assumes the heat capacities of the α and β phases to be negligibly different. Thus, this analysis is only valid for first order phase transitions.

Substituting equation (3) into equation (2) gives

$$\begin{aligned} x[-\Delta\bar{S}_1(T - T_1) + \Delta\mu_1^E] + y[-\Delta\bar{S}_2(T - T_2) + \Delta\mu_2^E] \\ + (1 - x - y)[-\Delta\bar{S}_3(T - T_3) + \Delta\mu_3^E] = 0, \end{aligned} \tag{4}$$

the solutions to which in terms of x, y and T gives the isobaric equal G surface. The excess Gibbs potential difference between the α and β phases at any T and p can be written as a weighted sum of excess chemical potential differences

$$\Delta\bar{G}^E = x\Delta\mu_1^E + y\Delta\mu_2^E + (1 - x - y)\Delta\mu_3^E. \tag{5}$$

Equation (4) can now be solved for temperature in terms of the measurable quantities, ΔS_is, T_is and the excess Gibbs energy

$$T = \frac{x(\Delta\bar{S}_1 T_1 - \Delta\bar{S}_3 T_3) + y(\Delta\bar{S}_2 T_2 - \Delta\bar{S}_3 T_3) + \Delta\bar{S}_3 T_3 + \Delta\bar{G}^E}{x(\Delta\bar{S}_1 - \Delta S_3) + y(\Delta\bar{S}_2 - \Delta\bar{S}_3) + \Delta\bar{S}_3}. \tag{6}$$

For a two component system the equal G line always lies inside the two phase coexistence region. This reasoning can be extended to a three component system (see figure 1), and the equal G line (the projection of the line resulting from the intersection of the two isothermal Gibbs energy surfaces in figure 1) will lie inside the two phase coexistence region defined by the phase surfaces as shown in figure 2. Since the resultant equal G surface must be between the two phase-boundary surfaces, the equal G surface will have minima or maxima that coincide with the minima or maxima of the two phase region. Moreover, since liquid crystals usually exhibit narrow two-phase regions (of the order of 0·1 K on a graph often spanning 50 K), the equal G surface by itself represents the phase diagram to reasonable accuracy.

The excess Gibbs potential, the quantitative estimate for the non-ideality of the phase diagram, may be determined using equation (6). Equation (6) can be solved for $\Delta\bar{G}^E$ to yield

$$\begin{aligned} \Delta\bar{G}^E = T[x(\Delta\bar{S}_1 - \Delta\bar{S}_3) + y(\Delta\bar{S}_2 - \Delta\bar{S}_3) + \Delta\bar{S}_3] \\ - [x(\Delta\bar{S}_1 T_1 - \Delta\bar{S}_3 T_3) + y(\bar{S}_2 T_2 - \Delta\bar{S}_3 T_3) + \Delta\bar{S}_3 T_3]. \end{aligned} \tag{7}$$

Knowledge of the transition entropies and temperatures and the experimental T, x and y phase diagram points allows ready calculation of $\Delta\bar{G}^E$. If $\Delta\bar{G}^E$ is zero, the phase diagram is ideal; if $\Delta\bar{G}^E$ is not zero, then the mixture exhibits intermolecular forces beyond those intermolecular forces between the pure components.

Of the several forms for $\Delta\bar{G}^E$ suggested by Lupis [6], we have considered

$$\bar{G}^E = A_{12}xy + A_{23}y(1 - x - y) + A_{13}x(1 - x - y), \tag{8}$$

$$\bar{G}^E = A_{12}xy + A_{23}y(1 - x - y) + A_{13}x(1 - x - y) + A_{123}xy(1 - x - y), \tag{9}$$

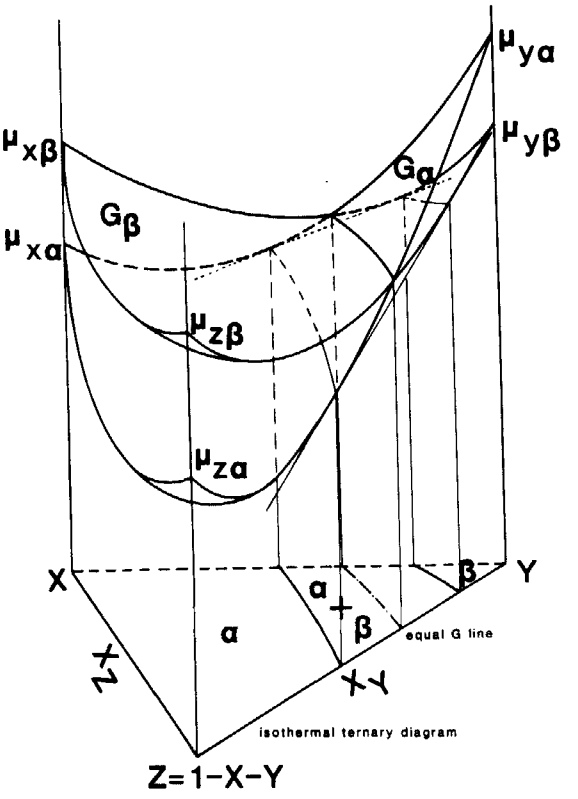

Figure 2. Idealized isobaric, ternary temperature–composition phase diagram showing the two phase coexistence region. The system drawn illustrates the case of each binary system exhibiting vapour–liquid or solid–solution two phase regions. The isothermal section shows the expected ternary isobaric and isothermal phase diagram. The surface depicted by the —·— intersection lines in the binary planes is the equal Gibbs surface estimating the phase diagram. For clarity, tie lines are not drawn but it is evident that the equal G surface will always lie inside the ternary two phase coexistence region. (Adapted from figure X-3 of [6].)

$$\bar{G}^{E} = A_{12}xy + A_{23}y(1 - x - y) + A_{13}x(1 - x - y) + xy(1 - x - y)[A_{1231}x + A_{1232}y + A_{1233}(1 - x - y)]. \quad (10)$$

These equations express the excess Gibbs potential for a single phase. For the equal G treatment, $\bar{G}^{E}_{\alpha} - \bar{G}^{E}_{\beta} = \Delta\bar{G}^{E}$; that is, the difference between the excess potentials in the two phases α and β is required. Since equations (8)–(10) are linear in the A parameters, the equations for $\Delta\bar{G}^{E}$ are identical to equations (8)–(10), except that the A parameters are replaced by the differences in the A parameters, $\Delta A = A_{ijkl\alpha} - A_{ijkl\beta}$.

Equation (8) corresponds to a linear sum of three non-ideal binary systems; equation (9) is a linear sum of three non-ideal binary systems plus an excess ternary energy; equation (10) is the same as equation (9) except the ternary interaction is further parameterized. All three forms satisfy the Gibbs–Duhem equation. For the study of liquid crystals, the second function appears most useful, since it allows for ternary effects without undue parameter overhead. The literature contains a wealth of non-ideal binary phase diagrams. Since some of these have been studied with the

equal G technique, the binary parameters derived from the ternary method can be compared with those derived from studying binary systems. They should be equal. Alternatively, the three binary parameters from previously analysed binary systems can be used to fit the ternary system with the ternary parameter alone.

Solving for these parameters from experimental data using any form for $\Delta\bar{G}^E$ involves only a simple least squares analysis, since the equal G equation is linear in the A parameters. In a more complicated analysis the parameters could be made dependent on temperature. It must be kept in mind that this analysis only gives, however, the differences in the parameter values between phases, e.g. $\Delta A_{12} = A_{12\alpha} - A_{12\beta}$. If some assumptions are made about the non-idealities of one of the coexisting phases, then the excess Gibbs potentials for each phase may individually be found (see the subsequent discussion of crystal–nematic transitions).

Given a specific functional form for the excess Gibbs potential in a specific phase, such as shown in equations (8)–(10), the excess chemical potentials in that phase can be derived according to equations given by Oonk [1]:

$$\mu_1^E = \bar{G}^E + (1 - x)(\partial\bar{G}^E/\partial x) - (y)(\partial\bar{G}^E/\partial y), \tag{11}$$

$$\mu_2^E = \bar{G}^E - (x)(\partial\bar{G}^E/\partial x) + (1 - y)(\partial\bar{G}^E/\partial y), \tag{12}$$

$$\mu_3^E = \bar{G}^E - (x)(\partial\bar{G}^E/\partial x) - (y)(\partial\bar{G}^E/\partial y). \tag{13}$$

The use of these equations will be illustrated when analysing the pure solid to nematic liquid transitions discussed later.

3. Experimental methods

Two systems of homologous 4,4′-di-*n*-alkyloxyazoxybenzenes were chosen for study. They are identified as 6–4–5 and 6–1–5, the number indicating the number of carbon atoms in the alkyl chain (e.g. 4 is 4,4′-di-*n*-butyloxyazoxybenzene). These were chosen for study since 6–4–5 is a nearly ideal system in the nematic–isotropic regions, whereas 6–1–5 is a highly non-ideal system.

A newly developed ternary contact method for optical thermal microscopy was used to gain general qualitative information about the phase diagrams exhibited by the systems [7]. Using this method we determined the approximate temperature ranges which were then studied and discovered minimum azeotrope-like behaviour in the 6–1–5 system. Both the crystal–nematic (C–N) and nematic–isotropic (N–I) transitions were studied; however, the bulk of our work concentrated on the N–I transition.

The N–I transition was studied primarily using microscopic thermal analysis with samples of known composition. Samples containing various known amounts of all three components were placed on a microscope slide and then melt-mixed. The resulting sample was then placed on a hot stage controlled by a Mettler FP52, usually a heating rate of 0·2 K min^{-1}, and viewed with an Olympus BH2 polarizing microscope. The stage was temperature calibrated using pure benzoic acid.

The C–N transition was studied using microscopic thermal analysis and differential scanning calorimetry. Since both the crystal and nematic phases were found to be highly birefringent, the detection of the phase change by optical microscopy was difficult. For this reason, the differential scanning calorimeter (Perkin–Elmer Model DSC 2) was used primarily. However, the experiment was further complicated by the presence of a second crystalline phase in the pentane homologue and solid-solution formation between the butyl and pentyl homologues.

4. Experimental results

The experimental temperature–composition phase diagram data for the two ternary systems are presented in tables 1 (6–1–5) and 2 (6–4–5). Included also in those tables are selected pure and binary data drawn from the literature.

Table 1. Transition temperatures for ternary and binary mixtures of 4,4′-di-*n*-alkyloxyazoxybenzenes, system 6–1–5. Component 6 is di-*n*-hexyl, 1 is dimethyl and 5 is di-*n*-pentyl. Included are transition temperatures and entropies for the pure components.

Molar fraction			Transition temperature/K					
'6'	'1'	'5'	C–N	N–I (*a*)	N–I (*b*)	ΔT (*c*)	$\Delta S/R$ (*d*)	$\Delta S/R$ (*e*)
0·082	0·410	0·508		395·35	395·45	0·10		
0·085	0·187	0·728	335·70	395·95	396·05	0·10		
0·114	0·589	0·297		397·35	398·15	0·80		
0·131	0·782	0·087	345·60	401·25	401·75	0·50		
0·178	0·695	0·127		398·25	398·55	0·30		
0·269	0·086	0·645	338·40	397·05	397·15	0·10		
0·284	0·253	0·463		395·75	395·85	0·10		
0·288	0·556	0·156	343·80	396·35	396·65	0·30		
0·289	0·413	0·298		395·75	395·95	0·20		
0·417	0·142	0·441		397·25	397·45	0·20		
0·492	0·155	0·353		397·05	397·25	0·20		
0·534	0·149	0·317		397·75	397·95	0·20		
0·701	0·187	0·112	348·10	397·75	398·05	0·30		
*	*	*	*	*	*	*		
1·000	0·000	0·000	352·75	402·30	402·30	0·00	13·827	0·313
0·800	0·200	0·000		396·90	397·50	0·60		
0·600	0·400	0·000		394·60	395·20	0·60		
0·400	0·600	0·000		394·70	395·30	0·60		
0·200	0·800	0·000		398·00	398·60	0·60		
0·000	1·000	0·000	392·65	408·50	408·50	0·00	9·276	0·169
0·000	0·800	0·200		397·60	398·40	0·80		
0·000	0·600	0·400		391·50	392·70	1·20		
0·000	0·400	0·600		389·20	390·00	0·80		
0·000	0·200	0·800		390·40	391·50	1·10		
0·000	0·000	1·000	348·65	396·40	396·40	0·00	5·033	0·220
0·200	0·000	0·800		397·00	397·60	0·60		
0·400	0·000	0·600		397·70	398·30	0·60		
0·600	0·000	0·400		397·70	398·30	0·60		
0·800	0·000	0·200		399·90	400·50	0·60		

Data below * are either pure or binary data taken from [5].

(*a*) Lower temperature limit of the nematic–isotropic coexistence region.

(*b*) Higher temperature limit of the nematic–isotropic coexistence region.

(*c*) The temperature coexistence range.

(*d*) The crystal–nematic transition entropy for the pure component.

(*e*) The nematic–isotropic transition entropy for the pure component.

5. Data analysis and discussion

5.1. *Nematic–isotropic transitions*

The N–I transition data were analysed using the four-parameter excess Gibbs energy function derived from equation (9). The nematic–isotropic excess Gibbs energy differences were extracted from the experimental data in tables 1 and 2 by using

Table 2. Transition temperatures for ternary and binary mixtures of 4,4′-di-*n*-alkyloxyazoxybenzenes, system 6–4–5. Component 6 is di-*n*-hexyl, 4 is di-*n*-butyl and 5 is di-*n*-pentyl. Included are transition temperatures and entropies for the pure components.

Molar fraction			Transition temperature/K					
'6'	'4'	'5'	C–N	N–I (*a*)	N–I (*b*)	ΔT (*c*)	$\Delta S/R$ (*d*)	$\Delta S/R$ (*e*)
0·387	0·286	0·327	352·35	402·35	402·55	0·2		
0·292	0·579	0·129	356·15	406·25	406·55	0·3		
0·612	0·185	0·203	351·15	401·35	401·55	0·2		
0·305	0·565	0·130	353·75	405·85	406·15	0·3		
0·412	0·422	0·166	351·25	403·95	404·25	0·3		
0·457	0·105	0·438	351·35	400·35	400·65	0·3		
0·082	0·386	0·532	359·15	402·85	403·05	0·2		
0·120	0·198	0·682	354·75	400·25	400·55	0·3		
0·781	0·121	0·098	360·35	400·95	401·25	0·3		
0·259	0·104	0·637	351·75	400·25	400·45	0·2		
0·100	0·613	0·287	362·65	406·25	406·65	0·4		
0·108	0·797	0·095		409·35	409·65	0·3		
*	*	*	*	*	*	*		
1·000	0·000	0·000	352·75	402·30	402·30	0·00	13·827	0·313
0·800	0·200	0·000		403·90	404·50	0·60		
0·600	0·400	0·000		405·40	406·00	0·60		
0·400	0·600	0·000		406·90	407·50	0·60		
0·200	0·800	0·000		408·10	408·70	0·60		
0·000	1·000	0·000	378·95	409·90	409·90	0·00	6·644	0·303
0·000	0·800	0·200		406·70	407·30	0·60		
0·000	0·600	0·400		404·20	404·80	0·60		
0·000	0·400	0·600		401·50	402·10	0·60		
0·000	0·200	0·800		399·10	399·70	0·60		
0·000	0·000	1·000	348·65	396·40	396·40	0·00	5·033	0·220
0·200	0·000	0·800		397·00	397·60	0·60		
0·400	0·000	0·600		397·70	398·30	0·60		
0·600	0·000	0·400		397·70	398·30	0·60		
0·800	0·000	0·200		399·90	400·50	0·60		

Data below * are either pure or binary data taken from [5].

(*a*) Lower temperature limit of the nematic–isotropic coexistence region.
(*b*) Higher temperature limit of the nematic–isotropic coexistence region.
(*c*) The temperature coexistence range.
(*d*) The crystal–nematic transition entropy for the pure component.
(*e*) The nematic–isotropic transition entropy for the pure component.

equation (7). The parameters obtained by least square analysis of the excess Gibbs energy data are presented in table 3. Also in table 3 are the transition temperatures and entropies of the pure materials which are necessary for the calculations. These parameters produce equal G surfaces, that is, the estimated N–I phase diagrams for the systems 6–4–5 and 6–1–5 shown in figures 3 and 5, respectively. In the figures the gridded lines represent the equal G surface, calculated using the parameters in table 3, and the circles are observed ternary system data points. Figures 4 and 6 present, respectively, the Gibbs energy surfaces for the 6–4–5 and 6–1–5 systems. Here also the gridded surface is the Gibbs energy and the circles are the data points derived from the experimental data via equation (7).

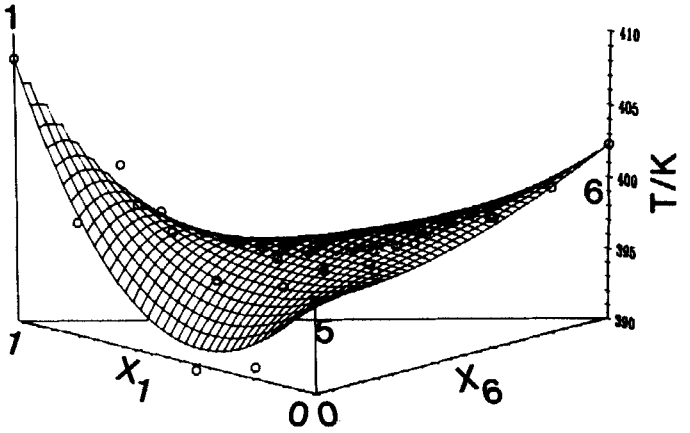

Figure 3. The nematic–isotropic equal G surface for ternary mixtures of 4,4′-di-*n*-alkyloxyazoxybenzenes, system 6–1–5. This surface lies between the upper and lower bounds of the nematic–isotropic coexistence region and, since this region is of the order of 0·5 K, the surface may be taken to be an accurate representation of the phase diagram. The gridded lines are the equal G surface calculated with the excess parameters fit to the data. The open circles are the observed clearing temperatures. The purely binary data was taken from Demus *et al.* (see table 2 and [5]). The values of the excess parameters A_{ijk}/R/K are (61–) −9·561, (–15) −7·732, (6–5) −2·134 and (615) 28·341, where the figures in parentheses are (ijk).

Table 3. Excess Gibbs energy parameters ΔA_{ijk} derived for the nematic–isotropic transition in the 6–1–5 and 6–4–5 systems. Component 6 is 4,4′-di-*n*-hexyloxyazobenzene, 1, 4 and 5 homologues are dimethyloxy, di-*n*-butyloxy and di-*n*-pentyloxy, respectively. Some of the binary parameters have been derived from other methods.

		Nematic–isotropic $\Delta A_{ijk}/R$/K parameters			
System	(*a*)	(*b*)	(*c*)	(*d*)	(*e*)
6–1	−9·561	−8·52	−9·76	−6·842	−9·619
5–1	−7·732	−1·06	−8·12	−9·144	X
4–5	−0·544	−3·29	1·07	X	X
6–4	0·096	−0·01	−1·23	X	X
6–5	−2·134[f]	−3·57	1·40	X	X
	−1·408[g]				
6–1–5	28·341				
6–4–5	2·787				

Sources:

(*a*) Four parameter fit to ternary system, this work.

(*b*) Estimated from an empirical correlation of transition enthalpy and carbon number of the homologue in question [8].

(*c*) Estimated from an empirical volume/parameter correlation [8].

(*d*) Calculated from binary phase data of Demus *et al.* using regular solution theory, $\Delta G^{E} = \Delta A_{ij} X(1 - X)$ [5, 8].

(*e*) As in (*d*); data from Hsu and Johnson [4 *a*].

(*f*) From 6–1–5 four parameter fit, this work.

(*g*) From 6–4–5 four parameter fit, this work.

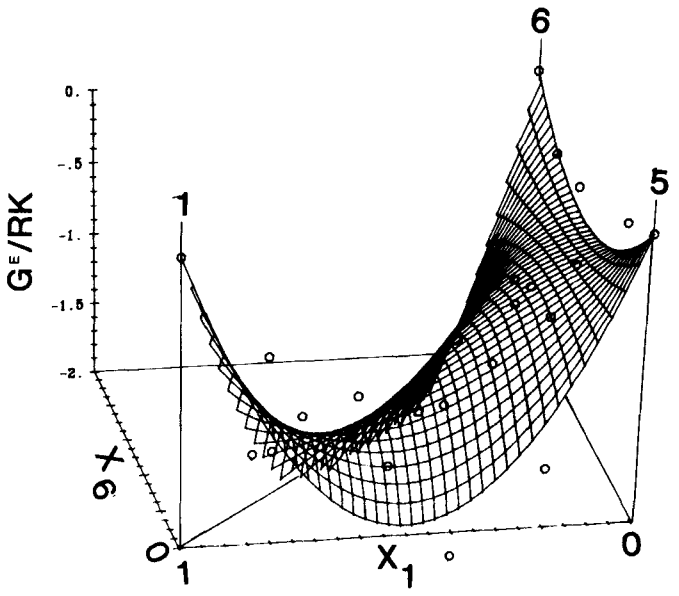

Figure 4. The excess Gibbs energy surface for the nematic–isotropic transitions region of ternary mixtures of 4,4′-di-*n*-alkyloxyazoxybenzenes, system 6–1–5. The surface quantitatively represents the non-ideality of the mixture. The gridded lines are the equal *G* surface calculated with the excess parameters fit to the data. The open circles are the excess energies derived from the observed phase diagram. The purely binary data were derived from [5].

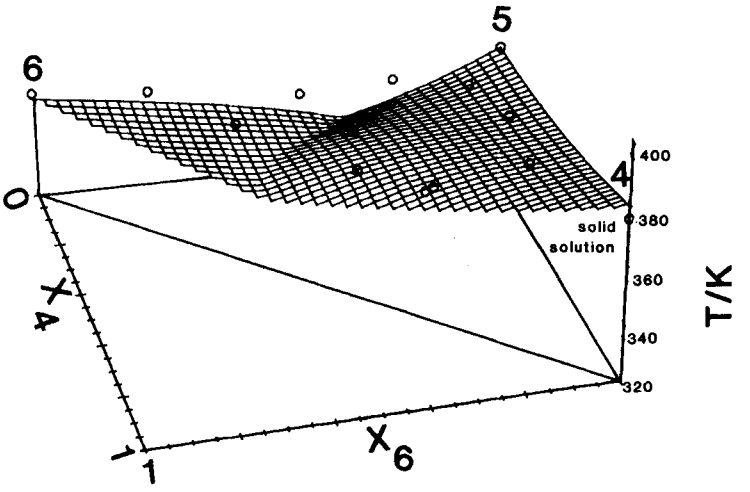

Figure 5. The crystal–nematic liquidus surfaces for ternary mixtures of 4,4′-di-*n*-alkyloxyazoxybenzenes, system 6–4–5. The gridded lines are the liquidus surface for the nematic phase in equilibrium with pure solid 6 and the equal *G* surface of the solid solution formed by 4–5 and 4–5–6 mixtures, each calculated with the excess parameters fit to the data. The open circles are the observed transition temperatures. The purely binary data were taken from Demus *et al.* (see table 1 and [8]). The values of the excess parameters A_{ijk}/R/K are (64–) 250, (−45) −125, (6–5) 164·5 and (645) 1450, where the numbers in parentheses are (ijk).

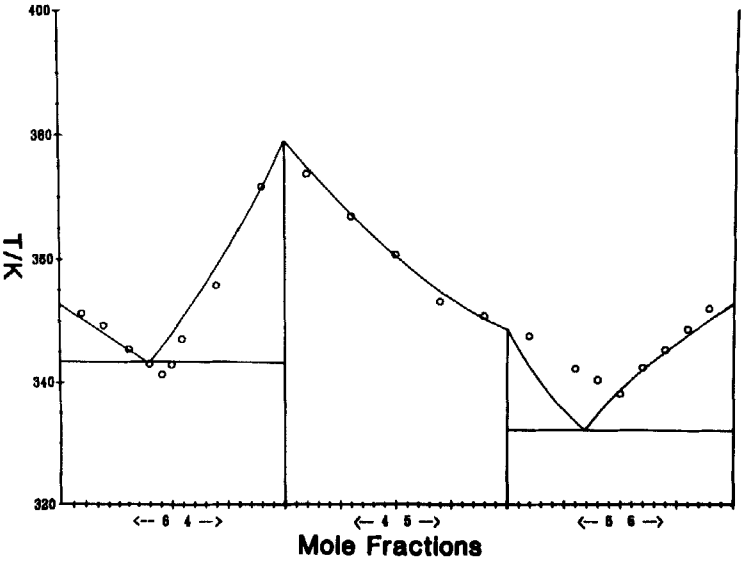

Figure 6. The crystal–nematic liquidus lines for the component binary mixtures of 4,4′-di-*n*-alkyloxyazoxybenzenes comprising the ternary system 6–4–5. The solid lines represent the liquidus surfaces calculated by fitting the three binary systems individually. The open circles are the binary data of Demus *et al.* (see table 1 and [5]).

5.1.1. *System 6–4–5*

The 6–4–5 ternary nematic–isotropic phase diagram as estimated by the equal Gibbs surface matches the experimental data quite well. The Gibbs surface has the shape shown in figure 2 where the deviation from the experiments points is on average ± 2 K. The reason for studying this system was that it should be ideal or at least close to ideal and the technique should work well. The excess Gibbs energy for this system, while small, generally never larger than $0{\cdot}2R$ K ($\approx 1{\cdot}7$/mol), is not zero. Thus, while the system is almost ideal, small additional energies which must result from some new intermolecular potentials present in the mixture. We find these interactions are more prevalent in 5-rich mixtures. The pentyloxy homologue 5 is somewhat anomalous in the series, in that its nematic–isotropic transition temperature and entropy, particularly the entropy, are not in agreement with the trends in these values set by the other homologues. On mixture, binary or ternary, this anomalous behaviour is apparently manifest by the introduction of the observed non-ideal behaviour particularly in 5-rich mixtures.

5.1.2. *System 6–1–5*

The 6–1–5 system was studied because it was known that the binary 6–1 and 5–1 systems were clearly non-ideal (since they exhibited minima). The binary 5–6 system also exhibits some non-ideality. The equal G surface shown in figure 3 estimates the experimental data well, though not as well for the 6–4–5 system. Note that a saddle ridge exists close to the 6–1 side of the diagram. The excess Gibbs surface and the derived data points are illustrated in figure 4. This ternary system is highly non-ideal. It should be noted that the non-ideality along the 6–5 edge is quite similar to that observed along the 6–5 edge in the 6–4–5 system. These similarities are to be expected. What is curious is that, although there are large intermolecular interactions along the

6–1 and 5–1 edges, the saddle ridge implies a reduction in those interactions when 5 is added to 6–1 mixtures and vice versa, although small amounts of 5 are more effective in reducing the 6–1 interactions then vice versa. the large interactions in this 6–1–5 system can be ascribed to significant size differences between the 1 homologue compared with the 5 and 6 homologues. How these size differences would account for these excess Gibbs energies should be addressable by a microscopic theory perhaps, modelled on the work of Sandler and of Tamura [9].

5.1.3. *System 6–4–5 and system 6–1–5 nematic–isotropic comparisons*

Table 3 contains the ΔA parameter values for the nematic–isotropic coexistence obtained by the equal G method applied to these ternary systems, as well as some parameters obtained from the study of pertinent binary systems. Column (*a*) of table 3 contains the binary parameter differences calculated using the four parameter $\Delta\bar{G}^{E}$ expression derived from equation (9). Columns (*d*) and (*e*) present binary parameters calculated using the regular solution approximation with $\Delta\bar{G}^{E} = \Delta A_{ij} X(1 - X)$ from the binary phase diagram data. The discrepancy between the ΔA_{61} values in (*d*) and (*e*) reflects the discrepancy in the original data. The binary values in columns (*b*) and (*c*) were obtained via the empirical procedure outlined in [8]. The agreement is quite satisfying, particularly the magnitudes. Special note should be made of the ΔA_{65} values calculated from each ternary system. The agreement is quite good, especially considering the relative insensitivity of the surfaces to variation in values of the parameters. It is not surprising to note that the ternary parameter for the nearly ideal 6–4–5 system is a factor of 10 less than that for the non-ideal 6–1–5 system. The intriguing, unanswered question at this point is, what form of microscopic theory could account for ternary intermolecular potentials?

5.2. *Crystal–nematic transitions*

The equal G analysis cannot be applied to phase transitions involving equilibria between a phase consisting of only one component (i.e. pure) and a phase composed of a mixture. In such a case the analysis must be made by studying the chemical potentials of the component existing in both phases. For pure solid–liquid mixture equilibria, the pure solid has a constant composition and the form of the chemical potential for a pure solid will differ from that of a liquid mixture:

$$\mu_{i\alpha} = \mu^{*}_{i\alpha} \tag{14}$$

$$\mu_{i\beta} = \mu^{*}_{i\beta} + RT \ln X_{i\beta}, \tag{15}$$

where α would refer to a pure solid phase and β to a liquid phase, here a nematic phase. The asterisk indicates the potential at a standard temperature and pressure. Isobaric and isothermal phase equilibria are, as usual, described by setting $\mu_{i\alpha}$ equal to $\mu_{i\beta}$. Again using the first order approximation (equation (3)), the equilibrium is described by

$$-\Delta\bar{S}_i(T - T_i) + \mu^{E}_{i\beta} = -RT \ln X_{i\beta}, \tag{16}$$

where it should be noted that $\Delta\bar{S}_i = \bar{S}_{i\alpha} - \bar{S}_{i\beta}$, the melting transition entropy, and that the pure solid phase (α) is assumed to be ideal with $\mu^{E}_{i\alpha}$ equal to zero, whereas the liquid mixture (nematic phase) may be non-ideal with $\mu^{E}_{i\beta}$ non-zero. Note that since the solid phase is assumed to be ideal, the non-ideality of the liquid phase in equilibrium

with it, can be determined absolutely, sign and magnitude. Equation (16) can be solved for the temperature to give

$$T = \frac{(\Delta\bar{S}_i T_i + \mu_{i\beta}^{E})}{(\Delta\bar{S}_i - R\ln X_{i\beta})}. \tag{17}$$

When dealing with ternary eutectic systems, three equations (17) are required, one for each leaf of the liquidus surface tied to the point $X_i = (1, T_i)$. (Figures illustrating such simple ternary eutectic systems are found in many introductory texts.) The temperature at the common intersection point of these three surfaces is the ternary eutectic temperature. Noting that the molar fractions must sum to unity, equation (16) can be solved for $x_{i\beta}$ and the $x_{i\beta}$s summed to give

$$\sum_i \exp\{[\Delta\bar{S}_i(T - T_i) - \mu_{i\beta}^{E}]/RT\} = 1 \qquad i = x, y, 1 - x - y. \tag{18}$$

This equation is a ternary version of the Schroeder–van Laar equation modified to include excess energies. The temperature which satisfies equation (18) is the ternary eutectic temperature. In an ideal system all excess chemical potentials are zero. In such a case equation (18) is easily solved for the eutectic temperature, knowing the transition temperatures and entropies of the three pure components. Comparing this calculated temperature with the experimentally observed ternary eutectic temperature, obtained readily by a ternary contact method, provides a quick check on the ideality of the system.

To deal with a non-ideal system, some form must again be chosen for the excess Gibbs energy. Once a firm is chosen, the individual excess chemical potentials may be derived from it by using equations (11)–(13). The excess chemical potentials were derived from the four-parameter Gibbs energy equation (9) and are

$$\begin{aligned}\mu_1^{E} = {} & A_{12}(1 - x)y - A_{23}(1 - x - y)y + A_{13}(1 - x)(1 - x - y) \\ & + A_{123}[xy(1 - x - y) + (1 - x)y(1 - 2x - y) - xy(1 - x - 2y)],\end{aligned} \tag{19}$$

$$\begin{aligned}\mu_2^{E} = {} & A_{12}x(1 - y) + A_{23}(1 - y)(1 - x - y) - A_{13}(1 - x - y)x \\ & + A_{123}[xy(1 - x - y) - xy(1 - 2x - y) + x(1 - y)(1 - x - 2y)],\end{aligned} \tag{20}$$

$$\mu_3^{E} = A_{12}xy + A_{23}(x + y)y + A_{13}(x + y)x + A_{123}xy(2x + 2y - 1). \tag{21}$$

To fit the ternary leaves, the excess chemical potential data was extracted from the phase diagram by solving equation (17) for μ_{iN}^{E}. Each ternary leaf would, in principle, provide an independent set of A_{ijk} parameters for the nematic phase. Presumably the three sets would yield comparable results.

5.2.1. *System 6–1–5*

Experimentally the sytem is observed to form a simple eutectic. The method of analysis differed in practice from that just outlined, however.The binary diagrams 6–1, 5–1 and 6–5 were analysed individually first to obtain the binary A_{ijN} parameters. With these parameters, the ternary μ_{iN}^{E} values were fitted with just the ternary A_{614N} parameter. The parameters obtained in this way are given in table 4 and the calculated surfaces agree with the experiment adequately, especially considering the paucity of experimental ternary data points.

Table 4. Absolute excess Gibbs energy parameters derived for the nematic phase by studying the crystal–nematic phase transitions in ternary systems of homologous dialkyloxyazoxybenzenes. The systems were 6–1–5 and 6–4–5, where the numeral stands for the homologue of that number of carbon atoms in the terminal alkyloxy group. The binary parameters were determined from analysis of the indicated binary system using the literature data. The ternary parameters were derived from the present ternary system data.

	System ijk	Nematic phase A_{ijk}/R/K
615	6–1	−9·3
	5–1	41·2
	6–5	164·5
	6–1–5	−2000
645	6–4	250
	4–5	−125(*a*)
	6–5	164·5
	6–4–5	1450

(*a*) Forms a solid solution.

The resulting values for the A_{ijk} C–N parameters are two orders of magnitude higher than those of the N–I transition. This is not surprising as the heats of transition for C–N are nearly two orders of magnitude higher than those for N–I.

5.2.2. *System 6–4–5*

The analysis of this system proved interesting because of the solid solution behaviour of the 4–5 mixtures. The results are illustrated in figure 5, which shows the locus of the solid solution–nematicus surface and the nematicus–pure solid component 6 surface. The diagram was analysed by considering the nematic to 4–5 solid solution surface to be extended into the ternary composition field as nematic to 4–5–6 solid solution surface until the ternary solid solution surface met the nematic–solid pure 6 leaf. We therefore looked at the diagram as a set of psuedo-binary diagrams with 6 as one component and the 4–5 solid solution as the other. The two parts of this pseudo-binary phase diagram are described by

$$T = \frac{\Delta\bar{S}_6\, T_6 + \mu^{E}_{6N}}{\Delta\bar{S}_6 - R\ln X_{6N}}, \tag{22}$$

$$T = \frac{X_{4S}\Delta\bar{S}_4\, T_4 + X_{5S}\Delta\bar{S}_5\, T_5 + X_{4N}\mu^{E}_{4N} + X_{5N}\mu^{E}_{5N}}{X_{4S}\Delta\bar{S}_4 + X_{5S}\Delta\bar{S}_5 - R\ln(1 - X_{6N})}, \tag{23}$$

where in each case the μ^{E}_{iN} is given by one of the appropriate equations (19)–(21). To derive equation (23) we start with equation (22), looking to modify equation (22) taking into account our assumption that the 4–5 solid solution can be treated as a pseudo-single component. Since $\Delta\bar{S}_6\, T_6$ represents the melting enthalpy for pure 6, for an arbitrary 4–5 mixture we take the melting enthalpy to be a composition weighted value given by $X_{4S}\,\Delta\bar{S}_4\, T_4 + X_{5S}\,\Delta\bar{S}_5\, T_5$. The transition entropy in the 4–5 mixture is also taken to be a composition weighted value, $X_{4S}\,\Delta\bar{S}_4 + X_{5S}\,\Delta\bar{S}_5$. For the excess Gibbs energy, we assume the solid phase to be ideal (hence the linear composition weighted enthalpy and entropy values), and assign any and all non-ideality to the nematic phase whose excess energy we also write as a simple composition weighted

sum, $X_{4N}\mu^{E}_{4N} + X_{5N}\mu^{E}_{5N}$. Substituting these expression into equation (22) yields equation (23) except that the replacement of the $R\ln X_{6N}$ term by $R\ln(1 - X_{6N})$ has to be justified. Our reasoning here is that we are approximating a solid solution in equilibrium with components 4 and 5, not component 6, and $1 - X_{6N}$ represents the composition that is not 6. Keeping in mind that since we are considering a system whose ratio of X_4 to X_5 is constant because we choose a value of X_{4S} to start the analysis of the system as psuedo-binary, at any point in the ternary system, $X_{4S}/X_{5S} = X_{4N}/X_{5N}$. Further, in the solid solution $X_{4S} + X_{5S} = 1$; thus $X_{4N} = X_{4N}/(X_{4N} + X_{5N})$. Making this substitution for compositions in equation (23) yields

$$T = \frac{X_{4N}\,\Delta\bar{S}_4\,T_4 + X_{5N}\,\Delta\bar{S}_5\,T_5 + X_{4N}(X_{4N} + X_{5N})\mu^{E}_{4N} + X_{5N}(X_{4N} + X_{5N})\mu^{E}_{5N}}{X_{4N}\,\Delta\bar{S}_4 + X_{5N}\,\Delta\bar{S}_5 - R(X_{4N} + X_{5N})\ln(X_{4N} + X_{5N})}, \tag{24}$$

with compositions only involving the nematic phase. This derivation is not strictly correct thermodynamically but is rationalized by its success in describing experiment, as illustrated in figure 5. It may also be noted that in the limit of $X_{6N} \to 0$, equation (23) (or equation (24)) reduces to that which describes just the 4–5 solid solution.

The actual analysis of the data was made by first estimating the binary parameters A_{56N} and A_{46N} from the 5–6 and 4–6 binary phase data. The ternary parameter A_{645N} and the parameter A_{45N} were found by analysing the solid solution–nematic experimental data. Figure 6 shows the fits to the simple binary phase diagram data. The A_{645N} ternary parameter was also obtained from the analysis of the component 6 leaf. The ternary parameter values were then averaged. All parameter values are given in table 4. These values are the absolute parameters for the nematic phase in this system.

The estimated phase diagram shown in figure 5 is in excellent agreement with the ternary experimental data. Figure 6 shows the three binary diagrams and the calculated results relative to the experimental data of Demus *et al.* [5]. It is somewhat surprising to see how non-ideal the nematic phases of these mixtures are. Curiously, the largest effects seem to appear in mixtures with molecules of similar size (6–5 and 6–4) yet 4–5 forms solid solutions. Also curious is the fact that the ternary parameters for 6–1–5 and 6–4–5 are of opposite sign although of the same magnitude, even when both systems are essentially simple eutectics. No explanation for these values is offered.

6. Summary and conclusions

The high quality of the data fits leads us to believe that the form chosen for the excess Gibbs energy (three excess binary interactions and one excess ternary interaction with no temperature dependence) accurately represents the microscopic behaviour of these ternary systems. That is, any molecular theory that attempts to explain the non-ideal behaviour of these systems should do so in terms of binary and ternary interactions.

Since the crystalline phase is assumed to be ideal, the parameters derived from analysing the C–N transition absolutely estimate the non-ideality of the nematic phase, not the difference in non-idealities between the nematic and crystalline phases. As mentioned, the latter values are given in table 4. These values indicate that the transition from nematic phase to isotropic phase is comparatively ideal (by at least an order of magnitude), but even the isotropic phase is not ideal as might be expected for a totally random phase.

The authors thank Mr Ned Freed of the Harvey Mudd College Mathematics Department for his assistance in using the MATHLIB program with which the three dimensional drawings presented in this paper were drawn. The authors also gratefully acknowledge the receipt of Mabel and Arnold Beckman Research Funds administered by Harvey Mudd College.

References

[1] OONK, H. A. J., 1981, *Phase Theory: Thermodynamics of Heterogeneous Equilibria* (Elsevier).
[2] VAN HECKE, G. R., 1985, *J. phys. Chem.*, **89**, 2058.
[3] ARNOLD, H., 1964, *Z. phys. Chem., Leipz.*, **225**, 45.
[4] HSU, E. C.-H., and JOHNSON, J. F., (a) 1973, *Molec. Crystals liq. Crystals* **20**, 177. (b) 1974, *Ibid.*, **25**, 145.
[5] DEMUS, D., FEITKAU, C. H., SCHUBERT, R., and KEHLEN, H., 1974, *Molec. Crystals liq. Crystals*, **25**, 215.
[6] LUPIS, C. H. P., 1983, *Chemical Thermodynamics of Materials* (North-Holland).
[7] NEBEL, G. E., and VAN HECKE, G. R., 1988, *Molec. Crystals liq. Crystals Lett.*, **5**, 171.
[8] VAN HECKE, G. R., 1979, *J. phys. Chem.*, **83**, 2344.
[9] SANDLER, S. I., 1985, *Fluid Phase Equilib.*, **19**, 233. TAMURA, T., 1988, Senior Thesis, Harvey Mudd College, California.